

Properties of Barium Strontium Titanate ($\text{Ba}_{1-x}\text{Sr}_x\text{TiO}_3$, $0 \leq x \leq 1$) Ceramics Prepared by Hydrothermal Process

MIN ZENG* and WEI FAN

State Key Laboratory Cultivation Base for Nonmetal Composites and Functional Materials, Southwest University of Science and Technology, Mianyang 621010, P.R. China

*Corresponding author: E-mail: zengmin@swust.edu.cn

Received: 9 May 2013;

Accepted: 29 October 2013;

Published online: 28 April 2014;

AJC-15076

Barium strontium titanate ($\text{Ba}_{1-x}\text{Sr}_x\text{TiO}_3$, $0 \leq x \leq 1$) was produced in a pressure vessel at 180 °C for 24 h using a facile hydrothermal technique, without any surfactants or templates, with an alkalescency solution. The as-prepared products were characterized by X-ray diffraction, transmission electron microscopy, the differential thermal analysis and thermo-gravimetry analysis and electron diffraction. The barium strontium titanate nanoparticles in various compositions were monodispersed without mutual aggregation and their average sizes were in the range of 50-80 nm. Furthermore, they showed highly crystallized perovskite phase over the whole composition range. The stoichiometry of the ($\text{Ba}_{1-x}\text{Sr}_x$) TiO_3 powder is discussed in relation to the mechanism of formation of the perovskite phase.

Keywords: $\text{Ba}_{1-x}\text{Sr}_x\text{TiO}_3$, Hydrothermal synthesis, Alkalescency.

INTRODUCTION

Barium strontium titanate ($\text{Ba}_{1-x}\text{Sr}_x\text{TiO}_3$, $x = 0-1$, BST) solid solutions demonstrate outstanding dielectric, ferroelectric, pyroelectric and piezoelectric properties. It is well-known that these properties critically depend on their chemical compositions and structural characteristics. That is, the electrical and electronic properties of barium strontium titanate can be modified according to the Sr content in the solid solution, crystallinity, particle size and shape and others. Thus far, there are three commonly used processing techniques to produce barium strontium titanate powders: conventional solid state¹⁻³, sol-gel⁴ and hydrothermal methods⁵⁻⁷. The solid-state technique requires a calcinations step at high temperature above 1000 °C to produce a crystalline solid solution and it can be contaminated due to repeated grinding. The obtained powder particles are usually big in size and wide in range⁸⁻⁹. The sol-gel technique is capable of producing nano-sized powders, but most of the starting chemicals are expensive, sensitive to moisture and require a particular processing environment to control the properties. The powder produced is normally amorphous^{4,10}.

Unlike both techniques, the hydrothermal synthesis is one of the most important techniques that has been previously reported, because of the several reasons including: (1) the production of fine particles with a narrow size distribution; (2) the direct preparation of crystalline productions without high-temperature calcinations compare with solid-state reaction;

(3) the presence of powders not needing to be milled before sintering, thus avoiding contamination; and (4) the production of spherical morphology particles. Previous reports have focused on the reaction of a titanium source such as titanium alkoxide (TTIP)⁶, titanium tetrachloride (TiCl_4), or a titanium oxide gel [$\text{Ti}(\text{OH})_4$] and used strong basicity sodium hydroxide or potassium hydroxide as alkaline mineralizer⁵. However, these raw materials may cause pollution. In order to meet the requirements and exponentially growing technological demand, there is a need to develop an eco-friendly approach for nano-materials hydrothermal synthesis that is devoid of using toxic chemicals in the synthesis protocol^{6-8,10}.

In this study, we carried out a low temperature hydrothermal reaction in a pressure vessel, without any surfactants or templates, with an alkalescency solution. TiO_2 source was P25- TiO_2 as it reacts faster than 100 % anatase or rutile⁸. The barium strontium titanate nanopowders are prepared at relatively low temperature 180 °C and show homogeneous, fine and well-dispersed characteristics with an average size about 50-80 nm.

EXPERIMENTAL

The preparation process of continuous hydrothermal synthesis barium strontium titanate particles is schematically shown in Fig. 1. First, a mixture of deionized water (100 mL), PEG-2000 (2 mL) and ammonia water (25 %, 6mL) was added to a 120 mL Teflon-lined autoclave to get a base solution.

$\text{Ba}(\text{OH})_2$, $\text{Sr}(\text{OH})_2$ and P25- TiO_2 (70 % anatase and 30 % rutile) with $(\text{Ba} + \text{Sr})/\text{Ti} = 1.2$ molar ratio was added to this base solution, it have a concentration of 0.1M. The system was sealed, heated rapidly to the reaction temperature (180 °C) and held for given times (24 h). After the reaction, the obtained precipitate was centrifuged at 3000 rpm for 5 min. The separation solution, chiefly consisted of PEG, $\text{Ba}(\text{OH})_2$ and ammonia water, will be reclaimed and recycled as a base solution. We have researched at least 9 times cycle synthesis results. The obtained precipitate was then dispersed into 100 mL of distilled water and centrifuged again. This washing process of the obtained precipitate was repeated three times. The barium ions in the clear layer of the solution were checked by adding 1 mL of aqueous solution of Na_2SO_4 (1 mol/L). After the whole centrifuge procedure, the formation of the white precipitate of BaSO_4 was not observed. Then, the three times centrifuge procedure was enough to remove the excess barium ions. The obtained precipitate was dried in an oven at 75 °C for 4 h. All of the chemicals used in this preparation were of reagent grade. The preparation process is schematically shown in Fig. 1.

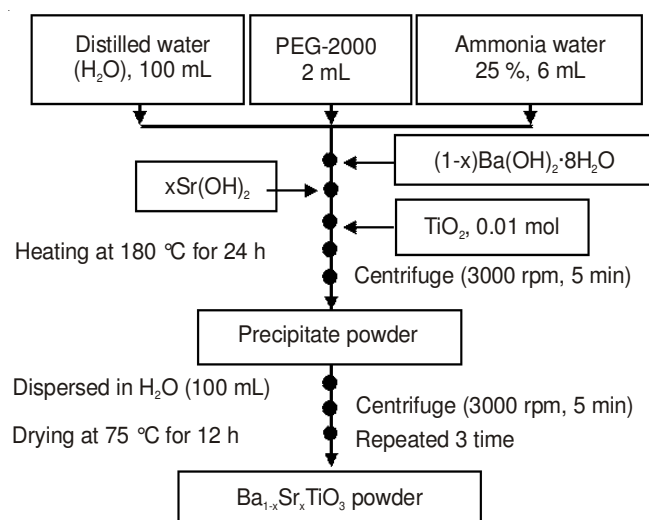


Fig. 1. Schematic representation of the preparation process of BaTiO_3 particles

Powder characterization: The X-ray diffraction patterns of the samples were measured by using Mac Science M18X-HF-SRA equipment. Copper was used as the target ($\text{Cu-K}\alpha$, 40 kV, 100 mA). An optical system of SS (scatter slit) = 1°, DS (divergence slit) = 1°, RS (receiving slit) = 0.30 mm and a graphite monochromator were used. Crystallite size of the barium strontium titanate powder was calculated from line-broadening of the (110) peak from the Scherrer's equation. The thermal decomposition and crystallization behaviors were studied with the differential thermal analysis and thermogravimetry analysis at a heating rate of 10 °C/min up to 1200 °C in air. The particle shape was observed by transmission electron microscope and field emission-secondary electron microscope (FE-SEM, JSM-6330, JEOL, Inc., Tokyo, Japan).

RESULTS AND DISCUSSION

X-ray diffraction: Fig. 2(I) shows XRD patterns of the as-prepared $\text{Ba}_{1-x}\text{Sr}_x\text{TiO}_3$ powders that hydrothermally

synthesized at 180 °C for 24 h: (a) $x = 0$, (b) $x = 0.2$, (c) $x = 0.5$, (d) $x = 0.8$ and (e) $x = 1$, respectively, with PEG-2000 and ammonia water as mineralizer. All diffraction peaks in Fig. 2(I) with different reaction conditions can be assigned to the highly crystallized perovskite phase barium strontium titanate, regardless of relative composition between Sr and Ba. And it was observed that barium strontium titanate nanocrystals can be hydrothermally synthesized only using ammonia water as mineralizer, in place of NaOH or KOH strong basic solution. Generally, use of aqueous ammonia solution in place of NaOH or KOH can be advantageous because: (a) ammonia does not have a tendency to get incorporated into the oxide matrix and (b) any residual ammonia entrained in barium strontium titanate powder can be easily driven off during drying the powder at low temperature. Due to these advantages, a systematic study was carried out for synthesizing barium strontium titanate using TiO_2 in barium hydroxide-ammonia medium. Generally, to prepare barium strontium titanate powder with smaller particle size, better particle size distribution and dispersity, barium strontium titanate powder was synthesised through the hydrothermal synthesis route, using polyethylene glycol 2000 (PEG2000) as surfactants. The coverage of PEG on the surface of particles resulted in alleviating of agglomeration because of the steric hindrance.

The insert in Fig. 2(II) represents the enlarged XRD patterns of the (110) peaks around $2\theta = 32^\circ$, the positions of (110) peaks were shifted to lower angle with increasing the Ba mol fraction, which is indicative that the lattice parameter of barium strontium titanate is gradually increased, as the content of Ba^{2+} ion, which is higher than Sr^{2+} , is increased from 0 to 100 %. Using Scherrer formula: $D = k\lambda / (B \cos \theta)$ where D is the size of powders, λ is the X-ray wavelength, B the FWHM of diffraction peak, θ the diffraction angle and the constant $k \approx 1$ and based on the half-width of (110) reflection of the observed X-ray data, the particle size of the barium strontium titanate powders can be calculated. The average diameters of the particles were (a) 55 nm, (b) 73 nm, (c) 65 nm, (d) 68 nm and (e) 50 nm, respectively. Fig. 2(II) plots the change of barium strontium titanate cell parameter as a function of Sr composition.

A linear increase of the cell parameter suggests that the complete solid solutions between SrTiO_3 and BaTiO_3 have been formed in the synthesized barium strontium titanate nanoparticles, according to the Vegard's law.

Thermal analysis: Fig. 3 shows TG-DTG-DTA curves of the $\text{Ba}_{0.5}\text{Sr}_{0.5}\text{TiO}_3$ precursor powder synthesized by a hydrothermal method at 180 °C for 24 h, with a heating rate of 10 °C/min from 30 to 1200 °C. It can be explained by the removal of physically adsorbed water below 200 °C with the 1.5 % weight loss in TG and the slow decrease in endothermic peak in DTA. There is no clear change (< 3 %) in TG and DTA between 200-1200 °C means that the precursor powders are the well-crystallized cubic phase of $\text{Ba}_{0.5}\text{Sr}_{0.5}\text{TiO}_3$.

Powder morphology: Fig. 4 shows the SEM images (I), TEM image (II), SAED pattern (III) and laser particle size analysis (IV) of the $\text{Ba}_{0.5}\text{Sr}_{0.5}\text{TiO}_3$ nanoparticles. As can be seen, the particle diameter could be calculated from the mean intercept length L , which was defined as L_L/N_L where L_L is the length of lineal intercepts per unit length of the test line and N_L is number of interceptions of features per unit length

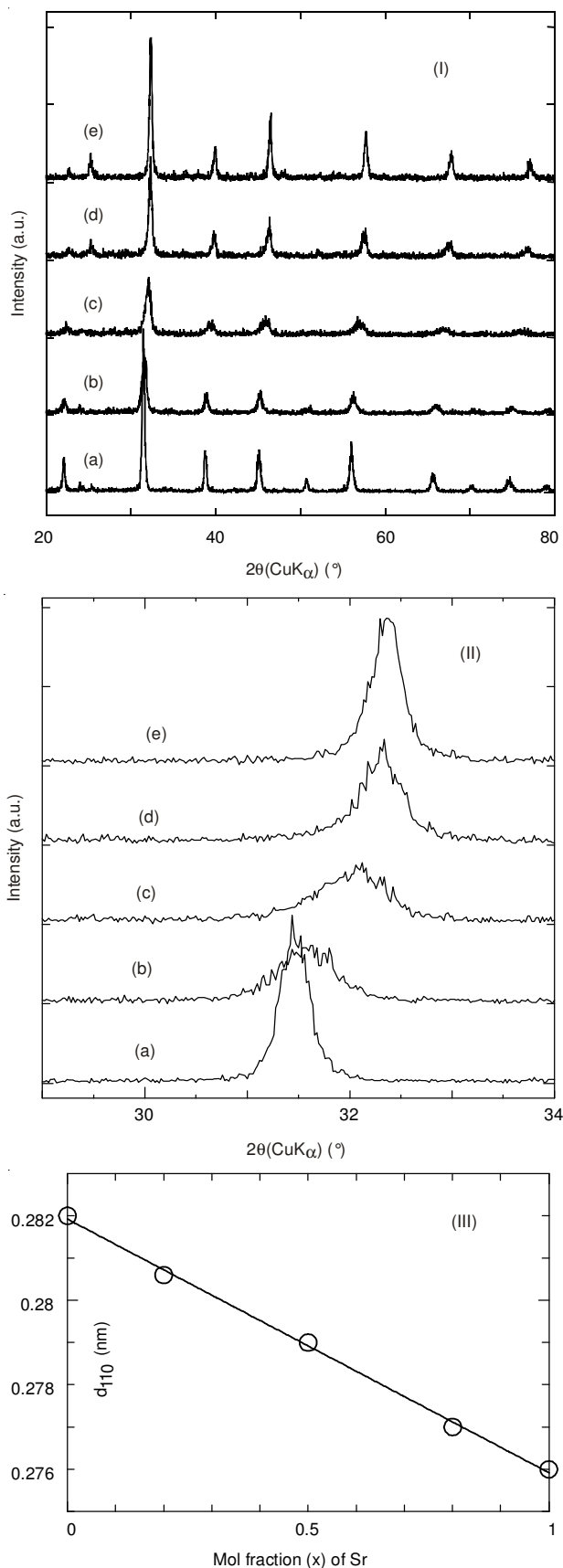


Fig. 2. (I) XRD patterns of the as-prepared $\text{Ba}_{1-x}\text{Sr}_x\text{TiO}_3$ powders synthesized by a hydrothermal method at 180°C for 24 h: (a) $x = 0$, (b) $x = 0.2$, (c) $x = 0.5$, (d) $x = 0.8$ and (e) $x = 1$, respectively. (II) a comparison of (110) diffraction peak positions for the patterns between $2\theta = 29\text{--}34^\circ$. Plot (III) describes the change of d_{110} as a function of Sr mol fraction in barium strontium titanate nanoparticles

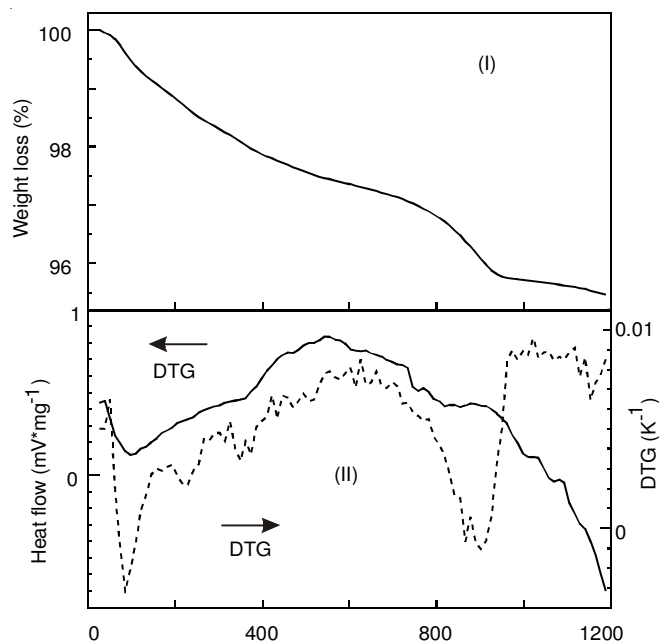


Fig. 3. DTA/TG traces of the $\text{Ba}_{0.5}\text{Sr}_{0.5}\text{TiO}_3$ precursor powder synthesized by a hydrothermal method at 180°C for 24 h

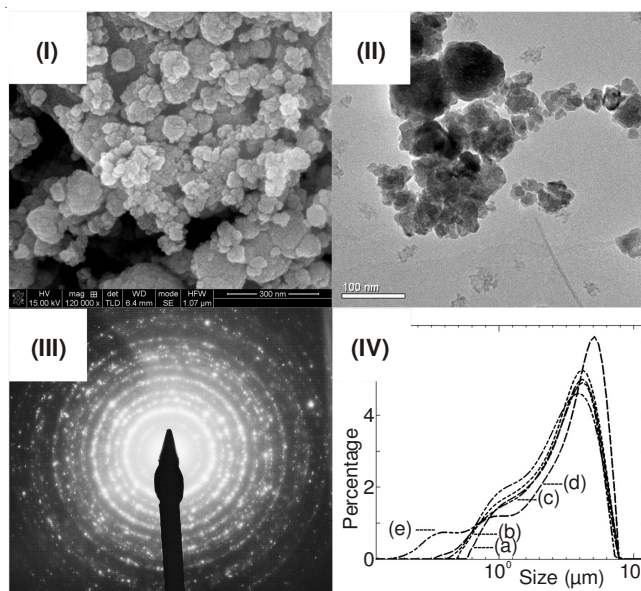


Fig. 4. (I) SEM images, (II) TEM image and (III) SAED pattern of the $\text{Ba}_{0.5}\text{Sr}_{0.5}\text{TiO}_3$ nanoparticles, (IV) Laser particle size analysis of $\text{Ba}_{1-x}\text{Sr}_x\text{TiO}_3$ powder products: (a) $x = 0$, (b) $x = 0.2$, (c) $x = 0.5$, (d) $x = 0.8$ and (e) $x = 1$, respectively

of test line. If the particle shape is sphere, the average diameter will be equal to $4L/3$. As shown in Fig. 4 (I) and (II), the average diameters of the particles were 60 nm and 50 nm, respectively. Furthermore, The SAED pattern [Fig. 4 (III)] reveals their polycrystalline nature. The d values estimated from this pattern did not reveal the presence of any other crystalline phases. The crystallite size of the as-synthesized powder is around 60 nm and is in good agreement with that obtained by XRD analysis, as shown in Figs. 2. and 4 (IV) shows laser particle size analysis of $\text{Ba}_{1-x}\text{Sr}_x\text{TiO}_3$ powder products: (a) $x = 0$, (b) $x = 0.2$, (c) $x = 0.5$, (d) $x = 0.8$ and (e) $x = 1$, respectively. Indicating its narrow particle size distribution as obtained from the Master sizer 2000, with a d_{50} value of 0.3-0.6 μm (*i.e.* 50 %

particles smaller than 0.3 μm). The ionic radii of Sr^{2+} are lower than that of Ba^{2+} . Due to its smaller size, Sr^{2+} ions can diffuse more easily than Ba^{2+} through the network of TiO_6 octahedra⁵, the average particle size decreased with an increasing amount of Sr^{2+} .

Conclusion

Barium strontium titanate was produced in a pressure vessel at 180 °C 24 h using a facile hydrothermal technique. The barium strontium titanate nanoparticles in various compositions were monodispersed without mutual aggregation and their average sizes were in the range of 50-80 nm. A linear increase of the cell parameter suggests that the complete solid solutions between SrTiO_3 and BaTiO_3 have been formed in the synthesized barium strontium titanate nanoparticles, according to the Vegard's law. Furthermore, they showed highly crystallized perovskite phase over the whole composition range. These results indicate that the hydrothermal synthesis with an alkalescency solution in this study is an eco-friendly approach for prepared barium strontium titanate nanomaterials.

ACKNOWLEDGEMENTS

This work is financially supported by the Project Sponsored by the Scientific Research Foundation for the Returned

Overseas Chinese Scholars, State Education Ministry [2011]-1568 and by the Open Project of State Key Laboratory Cultivation Base for Nonmetal Composites and Functional Materials (No. 11zxfk26).

REFERENCES

1. S. Tusseau-Nenez, J.-P. Ganne, M. Maglione, A. Morell, J.-C. Niepce and M. Pate, *J. Eur. Ceram. Soc.*, **24**, 3003 (2004).
2. H.V. Alexandru, C. Berbecaru, A. Ioachim, M.I. Toacsen, M.G. Banciu, L. Nedelcu and D. Ghetu, *Mater. Sci. Eng. B*, **109**, 152 (2004).
3. D. Zhang and P. Yu, *Asian J. Chem.*, **24**, 1715 (2012).
4. A. Ries, A.Z. Simoes, M. Cilense, M.A. Zaghete and J.A. Varela, *Mater. Charact.*, **50**, 217 (2003).
5. R.K. Roeder and E.B. Slamovich, *J. Am. Ceram. Soc.*, **82**, 1665 (1999).
6. M. Zeng, *Appl. Surf. Sci.*, **257**, 6636 (2011).
7. J. Liu, J. Wang and H. Zhou, *Asian J. Chem.*, **24**, 5055 (2012).
8. M. Zeng, N. Uekawa, T. Kojima and K. Kakegawa, *J. Mater. Res.*, **22**, 2631 (2007).
9. S.B. Deshpande, Y.B. Kholam, S.V. Bhoraskar, S.K. Date, S.R. Sainkar and H.S. Potdar, *Mater. Lett.*, **59**, 293 (2005).
10. M. Zeng, Y.J. Ma, S.W. Chen and C.H. Pei, *Mater. Sci. Forum*, **694**, 108 (2011).